

## Inorganic Chemistry

# Reactivity of [Cp\*Fe( $\eta^5$ -As<sub>5</sub>)] towards Carbenes, Silylenes and Germylenes

Stephan Reichl, Christoph Riesinger, Ravi Yadav, Alexey Y. Timoshkin, Peter W. Roesky, and Manfred Scheer\*

Dedicated to Professor Wolfgang A. Herrmann on the occasion of his 75<sup>th</sup> birthday

**Abstract:** The reaction behavior of [Cp\*Fe( $\eta^5$ -As<sub>5</sub>)] (**I**) (Cp\* = C<sub>5</sub>Me<sub>5</sub>) towards carbenes and their heavier analogs was investigated. The reaction of **I** with NHCs (NHCs = N-heterocyclic carbenes) results in the first substitution products of polyarsenic ligand complexes by NHCs [Cp\*Fe( $\eta^4$ -As<sub>5</sub>NHC)] (**1a**: NHC = IMe = 1,3,4,5-tetramethylimidazolin-2-ylidene, **1b**: NHC = IMes = 1,3-bis(2,4,6-trimethylphenyl)-imidazolin-2-ylidene). In contrast, the reaction of **I** with <sup>Et</sup>CAAC (<sup>Et</sup>CAAC = 2,6-diisopropylphenyl)-4,4-diethyl-2,2-dimethyl-pyrrolidin-5-ylidene) leads to a fragmentation and the formation of an unprecedented As<sub>6</sub>-sawhorse-type compound [As<sub>2</sub>(As<sup>Et</sup>CAAC)<sub>4</sub>] (**2**). The reaction of (LE)<sub>2</sub> (L = PhC(N<sup>t</sup>Bu)<sub>2</sub>; E = Si, Ge) with **I** resulted in a rearrangement and an insertion of LE fragments, forming unique silicon- (**4**: [Cp\*Fe( $\eta^4$ -As<sub>4</sub>SiL)], **5a**: [Cp\*Fe( $\eta^4$ -As<sub>6</sub>SiL)]) and germanium-containing (**5b**: [Cp\*Fe( $\eta^4$ -As<sub>6</sub>GeL)]) cyclic polyarsenic ligand complexes.

## Introduction

In 1991, *Arduengo* synthesized the first stable NHC.<sup>[1]</sup> This breakthrough in carbene chemistry opened the way for a multitude of further preparative milestones, combining inorganic and organic chemistry interests as well as providing numerous classes of new compounds, e.g. ligands in (a)symmetric catalysis.<sup>[2]</sup> *Bertrand* et al. advanced this research and synthesized a novel type of carbenes in 2005, the so-called CAACs (cyclic alkyl amino carbenes).<sup>[3]</sup> This further advancement influences the properties of carbenes in general, since CAACs reveal a smaller HOMO/LUMO gap in comparison to NHCs.<sup>[2b]</sup> Based on their electronic properties, they are stronger  $\sigma$ -donors and  $\pi$ -acceptors.<sup>[2a,b]</sup> Over the last three decades, a plethora of different NHCs and CAACs were prepared, featuring different substituents in order to tune their steric and electronic properties.<sup>[2a,b]</sup>

Scientific interest has also focused on the heavier homologs of carbenes. Their stabilization is generally more difficult and they often require special substituents such as amidinate substituents L (L = PhC(N<sup>t</sup>Bu)<sub>2</sub>). One class of such low-valent compounds of silicon and germanium are amidinate-stabilized chloro- or dimeric silylenes/germylenes.<sup>[4]</sup> In contrast to NHCs or CAACs, these compounds can also react as electrophiles (depending on the substrates).<sup>[5]</sup> Since the activation of white phosphorus, P<sub>4</sub>, by main group element compounds is an active topic in research,<sup>[6]</sup> it was obvious to combine both areas and investigate the reactivity of P<sub>4</sub> towards carbenes and (chloro)-silylenes or germylenes. Interesting results were reported inter alia by *G. Bertrand*,<sup>[7]</sup> *H. W. Roesky*,<sup>[8]</sup> *M. Driess*,<sup>[9]</sup> and *R. West* et al.<sup>[10]</sup>

As for the heavier homolog arsenic, the reactivity of yellow arsenic, As<sub>4</sub>, towards carbenes and their analogs has only been very rarely studied. Solely very few examples of arsenic-silicon or -germanium compounds, such as [As<sub>10</sub>(LSiN(TMS)<sub>2</sub>)<sub>3</sub>]<sup>[11]</sup> (TMS = SiMe<sub>3</sub>), [As<sub>2</sub>(SiL)<sub>2</sub>]<sup>[12]</sup> [As<sub>3</sub>(SiL)<sub>3</sub>]<sup>[12]</sup> (L = PhC(N<sup>t</sup>Bu)<sub>2</sub>) by our group, [As<sub>4</sub>(SiMe<sub>2</sub>)<sub>4</sub>]<sup>[10]</sup> by *R. West* as well as [As<sub>2</sub>(GeL'')<sub>2</sub>]<sup>[13]</sup> (L'' = CH-[CMeNDipp]<sub>2</sub>) by *H. Grützmacher* and *M. Driess*, have been reported so far (Scheme 1). Especially concerning the activation of As<sub>4</sub> by NHCs and CAACs as well as by germylenes, there is a significant scientific gap, although we could recently report some first results of the reaction between As<sub>4</sub> and CAACs.<sup>[14]</sup> This discrepancy is based on the difficult handling of yellow arsenic and to the lack of a

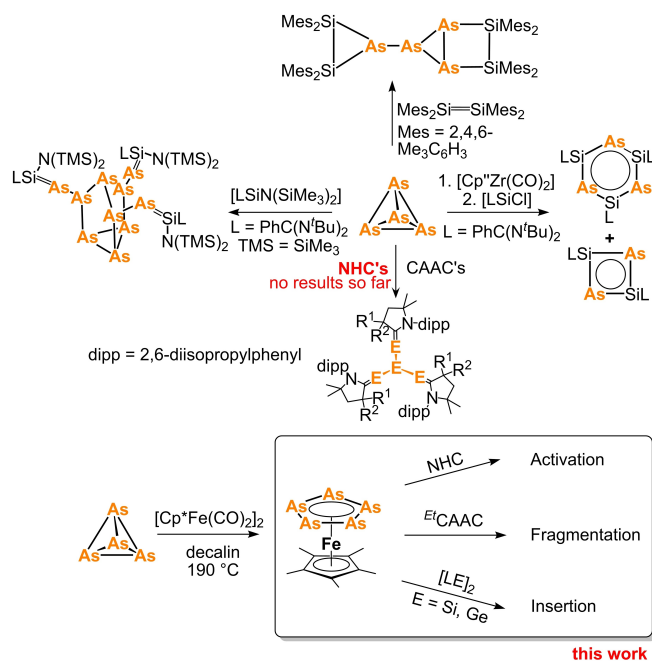
[\*] Dr. S. Reichl, M. Sc. C. Riesinger, Prof. Dr. M. Scheer  
Institute of Inorganic Chemistry, University of Regensburg  
93040 Regensburg (Germany)  
E-mail: manfred.scheer@chemie.uni-regensburg.de  
Homepage: <https://www.uni-regensburg.de/chemie-pharmazie/anorganische-chemie-scheer/startseite/index.html>

Dr. R. Yadav, Prof. Dr. P. W. Roesky  
Institute of Inorganic Chemistry, Karlsruhe Institute of Technology (KIT)  
Engesserstraße 15, 76131 Karlsruhe (Germany)

Dr. R. Yadav  
School of Chemistry, Indian Institute of Science Education and Research Thiruvananthapuram  
Thiruvananthapuram-695551, Kerala (India)

Prof. A. Y. Timoshkin 0000-0002-1932-6647  
Institute of Chemistry, Saint Petersburg State University  
Universitetskaya emb. 7/9, 199034 St. Petersburg (Russia)  
Homepage: 0000-0002-1932-6647

© 2023 The Authors. *Angewandte Chemie International Edition* published by Wiley-VCH GmbH. This is an open access article under the terms of the Creative Commons Attribution Non-Commercial NoDerivs License, which permits use and distribution in any medium, provided the original work is properly cited, the use is non-commercial and no modifications or adaptations are made.



**Scheme 1.** Reactivity of yellow arsenic ( $\text{As}_4$ ) (top) as well as  $[\text{Cp}^*\text{Fe}(\eta^5\text{-As}_5)]$  (**I**) (bottom) towards carbenes and their analogs.

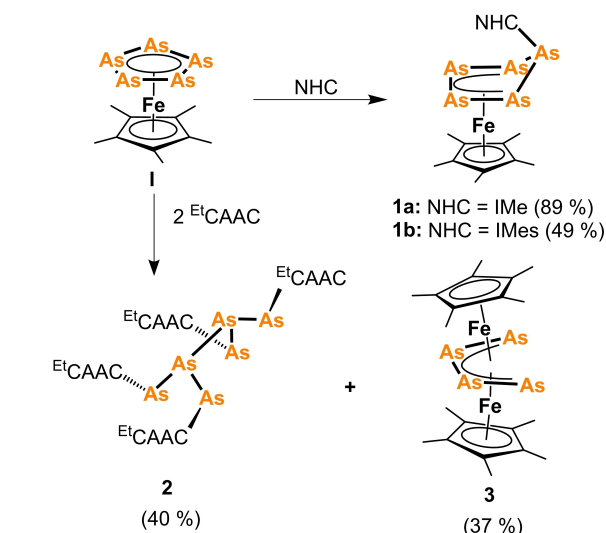
convenient NMR-active nucleus to monitor reactions in the case of  $\text{As}_4$  conversions in comparison to  $\text{P}_4$  reactions. An interesting transition metal derivative of  $\text{As}_4$  is pentaarsaferrocene  $[\text{Cp}^*\text{Fe}(\eta^5\text{-As}_5)]$  (**I**,  $\text{Cp}^* = \text{C}_5\text{Me}_5$ ), which is a light-stable compound and much easier to handle than  $\text{As}_4$ . Interestingly, its reactivity towards low-valent group 14-containing compounds has not been investigated yet.  $[\text{Cp}^*\text{Fe}(\eta^5\text{-As}_5)]$  (**I**) can be prepared with little effort and represents one of the very few end-deck  $\text{As}_n$  ligand complexes, featuring a versatile and sterically accessible *cyclo-As*<sub>5</sub> moiety.

Inspired by the reactivity of  $[\text{Cp}^*\text{Fe}(\eta^5\text{-P}_5)]$  (**II**) towards carbenes,<sup>[15]</sup>  $\text{LECl}$  and  $(\text{LE})_2$  ( $\text{E} = \text{Si}, \text{Ge}$ ;  $\text{L} = \text{PhC}(\text{N}^i\text{Bu})_2$ )<sup>[16][17]</sup> the question arises if the reaction behavior of the As derivative (**I**) would be similar or different in comparison to its lighter P-homolog (**II**).

Herein we report the reactivity of **I** towards selected NHCs and CAACs as well as low-valent dimeric silylenes and germylenes leading to unprecedented polyarsenic-silicon and -germanium complexes as well as a unique CAAC-stabilized  $\text{As}_6$  sawhorse-type molecule.

## Results and Discussion

By mixing an equimolar solution of **I** with the NHC IMe (1,3,4,5-tetramethylimidazolin-2-ylidene) in THF at room temperature, an immediate change in color from green to red/brownish occurred. After workup (cf. SI), brown crystals of  $[\text{Cp}^*\text{Fe}(\eta^4\text{-As}_5\text{IMe})]$  (**1a**) are obtained in 89% yield (Scheme 2). Single crystal X-ray structure analysis of **1a** reveals an  $\eta^4\text{-As}_5\text{IMe}$  moiety, featuring an envelope geometry with four arsenic atoms in the plane coordinating



**Scheme 2.** Reactivity of  $[\text{Cp}^*\text{Fe}(\eta^5\text{-As}_5)]$  (**I**) towards IMe, IMes and  $\text{EtCAAC}$ . Yields are given in parentheses.

towards the  $\text{Cp}^*\text{Fe}$  fragment, with the arsenic atom bearing the NHC that is out of the plane (Figure 1). The newly formed As–C bond is with 1.982(3) Å in accordance with an arsenic-carbon single bond.<sup>[18]</sup> The As–As bond lengths of 2.3623(6) – 2.4376(3) Å are within the range of a single and a double bond.<sup>[18,19]</sup> In contrast to previous investigations on the reactivity of  $[\text{Cp}^*\text{Fe}(\eta^5\text{-P}_5)]$  towards  $\text{IMe}^{[15]}$  for which an equilibrium is observed in solution, here, the equilibrium is exclusively shifted towards the formation of  $[\text{Cp}^*\text{Fe}(\eta^4\text{-As}_5\text{IMe})]$  (**1a**), since no starting material **I** can be monitored in the  $^1\text{H}$  NMR spectrum of the reaction solution (Figure S1). The same applies when using the weaker donating IMes (1,3-bis(2,4,6-trimethylphenyl)-imidazolin-2-ylidene). The color of the reaction solution changes drastically and crystals of  $[\text{Cp}^*\text{Fe}(\eta^4\text{-As}_5\text{IMes})]$  (**1b**) can be obtained at  $-80^\circ\text{C}$ , losing crystallinity at higher temperatures. Quantum

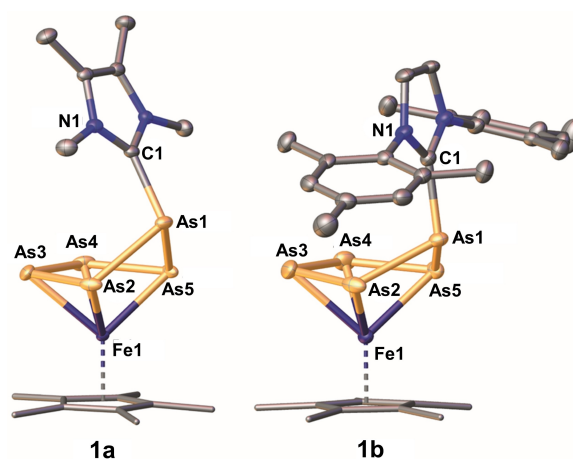


**Figure 1.** Molecular structures of **1a** and **1b** in the solid state. Hydrogen atoms are omitted for clarity. The  $\text{Cp}^*$  ligands are drawn in a wire frame model. Thermal ellipsoids are drawn at 50% probability.

chemical computations at the B3LYP/6-31G\*\* level of theory indicate that the reaction of **I** with both NHCs is exothermic and exergonic at room temperature (Table 1); interaction with IMes is by 33 kJ mol<sup>-1</sup> more energetically favorable than with IMe. The standard Gibbs energies for both processes are exergonic at 298.15 K. The equilibrium is shifted to the formation of **1a** and **1b** (the respective values of the equilibrium constants are 3.6 · 10<sup>5</sup> and 2.8 · 10<sup>7</sup>), which is in qualitative agreement with experimental observations.

XRD reveals isostructural complexes such as the phosphorus analogs<sup>[14]</sup> with similar bond lengths in **1a,b** (Table S3 and S5). A minor difference in the solid-state structure is given in the envelope structure of the As<sub>5</sub> unit (Figure 1). Whereas in **1a** the arsenic atom bearing the NHC is bent out of the plane with an angle of 56.59(2)°, the corresponding angle in **1b** is with 41.59(3)° smaller. Notably, complexes **1a** and **1b** represent the first NHC-functionalized polyarsenide ligand complexes.

Replacing the NHCs with <sup>Et</sup>CAAC (2,6-diisopropylphenyl)-4,4-diethyl-2,2-dimethyl-pyrrolidin-5-ylidene) in the reaction setup leads to an intensive bright green color of the reaction mixture at -80 °C in THF (Scheme 2). While warming the reaction mixture to room temperature, the color changed from green to red. NMR spectroscopy and mass spectrometry of the reaction solution indicate the presence of the starting material **I** and one additional Cp\*Fe- as well as one <sup>Et</sup>CAAC-containing species, respectively. Using two equivalents of <sup>Et</sup>CAAC leads to the disappearance of complex **I**. After consecutive workup and crystallization (cf. SI), the two compounds As<sub>6</sub>(<sup>Et</sup>CAAC)<sub>4</sub> (**2**) and [(Cp\*Fe)<sub>2</sub>[μ,η<sup>4,4</sup>-As<sub>4</sub>]] (**3**) are isolated in 40 and 37 % yields, respectively (Scheme 2).

According to DFT computations, the process of the interaction of **I** with two equivalents of <sup>Et</sup>CAAC under formation of **2** and **3** is energetically favorable and highly exergonic at room temperature (Table 1). The analogous process with the formation of two As(As<sup>Et</sup>CAAC)<sub>2</sub> radicals instead of **2** by the reaction of **I** with two equivalents of <sup>Et</sup>CAAC is exergonic by 30 kJ mol<sup>-1</sup>, and the dimerization of

two radicals As(As<sup>Et</sup>CAAC)<sub>2</sub> with the formation of **2** is highly exergonic. Thus, the *in situ* generation of the radical is thermodynamically allowed, but the recombination of the radicals is much more favorable.

Single crystal X-ray structure analysis of **2** reveals a unique <sup>Et</sup>CAAC-stabilized As<sub>6</sub> sawhorse type molecule (Figure 2). All As–As bond lengths in **2** of 2.4313(3) – 2.4418(3) Å are very close to a single bond.<sup>[18]</sup> The As1–As2 bond length is 2.4418(3) Å, showing no significant elongation in comparison to the other As–As bond lengths. The corresponding As–C distances of 1.865(2)/1.869(2) Å are in between a single and double bond.<sup>[17,19]</sup> The wingtip arsenic atoms As4 and As3/As5 and As6 are almost at right angles to each other with 96.76(2)°/95.93(2)° and are linked via As1/As 2, respectively. With a torsion angle of 57.49(1)° (As1–As3–As4 towards As2–As5–As6 plane), a gauche arrangement is present within the sawhorse-type structure in the solid state. Compound **2** is obtained as yellow plates and is soluble in *n*-hexane, toluene, diethyl-ether as well as THF and shows decomposition to grey arsenic when exposed to light in solution, but can be stored under inert gas atmosphere as a solid at room temperature. <sup>1</sup>H NMR spectroscopic investigations of **2** exhibit signals for four <sup>Et</sup>CAAC-substituents (Figure S3), suggesting a gauche-like arrangement of the CAAC groups in solution, making them chemically inequivalent and inhibiting a rotation. Mass spectrometric measurements of **2** reveal a peak corresponding to the cation [As<sub>3</sub><sup>Et</sup>CAAC<sub>2</sub>]<sup>+</sup>, suggesting the formation of **2** via the dimerization of two [As<sub>3</sub><sup>Et</sup>CAAC<sub>2</sub>]<sup>·</sup> radicals, which might also be an explanation for the intense bright color when mixing **I** with <sup>Et</sup>CAAC at -80 °C. Notably, related but anionic species of the type [(R<sub>2</sub>C=P)<sub>2</sub>Pn]<sup>-</sup> (Pn = N, P, As, Sb; R = H, Me, CF<sub>3</sub>, SiH<sub>3</sub>, SiMe<sub>3</sub>, SiF<sub>3</sub>) are known in literature.<sup>[20]</sup> Interestingly, an EPR investigation of the reaction mixture at -80 °C shows no signals and, regardless of numerous attempts, no intermediate could be isolated at the work-up at that low temperature. The dissociation of **2** into two radicals by breaking the As–As bond is endothermic by 313 kJ mol<sup>-1</sup> (per mol of **2**). Thus, this process is not thermodynamically favorable at room temperature. The equilibrium constant for the dissociation is only 10<sup>-38</sup> at 298.15 K which implies a very low concentration of radicals

**Table 1:** Standard gas phase reaction enthalpies ΔH<sup>o</sup><sub>298</sub>, Gibbs energies ΔG<sup>o</sup><sub>298</sub> in kJ mol<sup>-1</sup>, and reaction entropies ΔS<sup>o</sup><sub>298</sub>, J mol<sup>-1</sup> K<sup>-1</sup> of selected reactions. B3LYP/6-31G\*\* level of theory.

Reaction	ΔH <sup>o</sup> <sub>298</sub>	ΔS <sup>o</sup> <sub>298</sub>	ΔG <sup>o</sup> <sub>298</sub>
<b>I</b> + IMe = <b>1a</b>	-83.9	-174.8	-31.7
<b>I</b> + IMes = <b>1b</b>	-116.8	-249.1	-42.5
<b>I</b> + <sup>Et</sup> CAAC = <b>1c</b>	-96.5	-221.5	-30.4
2 <b>I</b> + 4 <sup>Et</sup> CAAC = <b>2</b> + <b>3</b>	-517.9	-918.2	-244.1
2 <b>I</b> + 4 IMe = 2 <b>IMe</b> + <b>3</b>	-114.7	-682.6	88.8
2 <b>I</b> + 4 IMes = 2 <b>IMes</b> + <b>3</b>	-146.8	-1005.2	152.9
2 = 2 As( <sup>Et</sup> AsCAAC) <sub>2</sub>	312.7	332.8	213.5
<b>II</b> + IMe = <b>1aP</b>	-39.2	-170.3	11.6
<b>II</b> + IMes = <b>1bP</b>	-27.9	-192.1	29.4
<b>II</b> + <sup>Et</sup> CAAC = <b>1'</b>	-4.9	-202.6	55.5
2 <b>II</b> + 4 <sup>Et</sup> CAAC = 2 <b>P</b> + 3 <b>P</b>	-202.3	-779.2	30.0
2 <b>II</b> + 4 IMe = 2 <b>P</b> IMe + <b>3</b>	-63.4	-617.1	120.6
2 <b>II</b> + 4 IMes = 2 <b>P</b> IMes + <b>3</b>	87.7	-840.4	338.2
2 <b>P</b> = 2 P( <sup>Et</sup> CAAC) <sub>2</sub>	28.2	292.7	-59.1

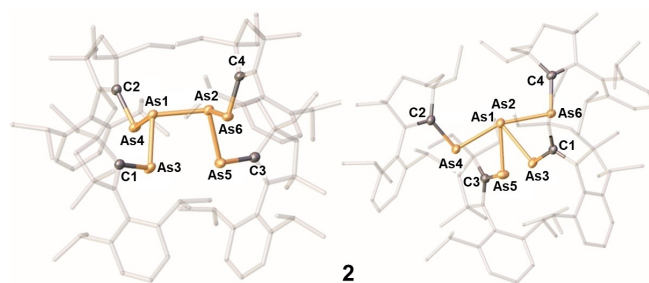


**Figure 2.** Molecular structure of **2** in the solid state (left: side view; right: view along the As1–As2 bond). Hydrogen atoms are omitted for clarity. The <sup>Et</sup>CAAC molecules are drawn in a wire frame model and the translucent is set to 20% for clarity. Thermal ellipsoids are drawn at 50 % probability.

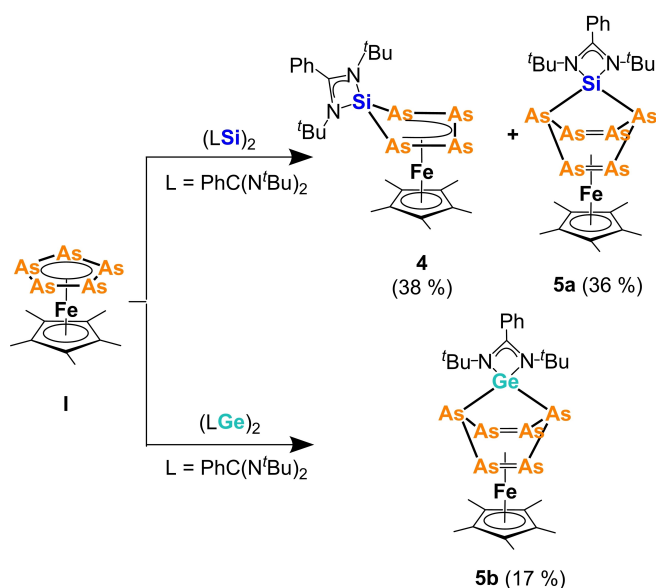
in the gas phase equilibrium, in agreement with the absence of signals in the EPR spectrum in solution.

Compound **3** represents an As<sub>4</sub> triple decker complex. Similar complexes with bulkier substituted Cp ligands are reported in literature.<sup>[20]</sup> However, the synthetic route given in Scheme 2 offers a way to its Cp\* derivative, which was not accessible so far.

Unfortunately, crystals of **3** were of limited quality due to twinning and, independent of many attempts, it was not possible to obtain suitable crystals for better measurements. Therefore, the bond features are not discussed in detail. However, the atomic connectivity of **3** could be unequivocally determined and the unit cell parameters are given (Figure S16, Table S2).

In contrast, the reaction of the phosphorus complex [Cp\*Fe(η<sup>5</sup>-P<sub>3</sub>)] (**II**) with EtCAAC does not lead to a fragmentation. Instead, the carbene adduct [Cp\*Fe(η<sup>4</sup>-P<sub>3</sub>EtCAAC)] (**1'**) (Figure S20) is formed. Similar to a previous report on NHC interactions with **II**,<sup>[15]</sup> an equilibrium between **II** and EtCAAC is observed. VT <sup>31</sup>P{<sup>1</sup>H} NMR investigations in toluene-d<sub>8</sub> show a ratio of **II** to **1'** of 1:5 (193 K) to 1:7 (313 K) (Figure S20) (decomposition above 313 K). However, a phosphorus analog of **2** cannot be detected. DFT computations indicate that the process of **2P** and **3P** formation is endergonic (Table 1).

Next, we compared the reaction behavior of **I** and **II** towards dimeric tetrylenes.<sup>[16,17]</sup> Therefore, the reactivity of **I** towards (LE)<sub>2</sub>,<sup>[4d,e]</sup> respectively, (L = PhC(N<sup>t</sup>Bu)<sub>2</sub>; E = Si, Ge) was investigated (Scheme 3). The reaction of **I** with (LSi)<sub>2</sub> (and LSiCl; cf. SI) at -80 °C leads to an immediate change in color from green to red. After warming the mixture to room temperature overnight and consecutive workup (cf. SI), the complexes [Cp\*Fe(η<sup>4</sup>-As<sub>4</sub>SiL)] (**4**) and [Cp\*Fe(η<sup>4</sup>-As<sub>6</sub>SiL)] (**5a**) were isolated as dark green blocks (**4**) and plates (**5a**), respectively (Scheme 3).



**Scheme 3.** Reactivity of [Cp\*Fe(η<sup>5</sup>-As<sub>5</sub>)] (**I**) towards (LSi)<sub>2</sub> and (LGe)<sub>2</sub> (L = PhC(N<sup>t</sup>Bu)<sub>2</sub>). Yields are given in parentheses.

The solid-state structure of **4** (Figure 3) shows the formation of a unique envelope [As<sub>4</sub>SiL] moiety, coordinating in an η<sup>4</sup> fashion by four arsenic atoms to the [Cp\*Fe] fragment (Figure 3). The silicon arsenic bond lengths of 2.2855(7) Å (As1–Si1) to 2.2792(7) Å (As4–Si1) are in between a single and a double bond.<sup>[18,19]</sup> The As–As bond lengths (2.3579(4) Å to 2.3866(4) Å) exhibit double bond character.<sup>[19]</sup> The molecular structure **5a** in the solid state of (Figure S18) exhibits an unprecedented norbornadiene-like As<sub>6</sub>SiL ligand composed by two arsenic dumbbells (d(As2–As3) = 2.3751(9) Å) coordinating to the Cp\*Fe moiety and bridged by an As<sub>2</sub>SiL fragment (Figure S17). The arsenic-silicon distance of 2.3055(15)/2.3047(17) Å is comparable to that in **4**, representing a shortened single bond.<sup>[18]</sup>

<sup>29</sup>Si{<sup>1</sup>H} NMR investigations of the reaction mixture show a selective reaction and solely two silicon-containing species, **4** and **5a** (Figure S21). The singlet at δ = 45.9 ppm can be attributed to **4** with a similar NMR shift to the analogous phosphorus complex.<sup>[16]</sup> The signal at δ = 85.9 ppm in the <sup>29</sup>Si{<sup>1</sup>H} NMR spectrum (Figure S12) represents compound **5a**. The latter complex can be selectively isolated after crystallization from THF/*n*-pentane and storage at 8 °C as dark green plates in 36% yield. <sup>1</sup>H and <sup>29</sup>Si{<sup>1</sup>H} NMR investigations of the isolated crystals confirm the previous assignment of complex **5a**. Due to the slightly different solubility of **4** and **5a**, complex **4** can be separated from **5a** by consecutive workup (cf. SI). <sup>29</sup>Si{<sup>1</sup>H} NMR spectroscopy of the obtained crystals of **4** reveals solely one singlet at δ = 46.1 ppm (Figure S11). However, <sup>1</sup>H and <sup>13</sup>C NMR spectra of **4** indicate the presence of a second Cp\*-containing species, which can be attributed to the starting material **I**, as a presumable decomposition product (Figure S5 and S9). Due to the similar solubility of **4** and **I** as well as the light sensitivity of **4** in solution, the latter can unfortunately not be obtained in an analytically pure form.

To the best of our knowledge, both complexes **4a** and **5a** represent the first five-membered As<sub>4</sub>SiL<sup>[21]</sup> as well as the

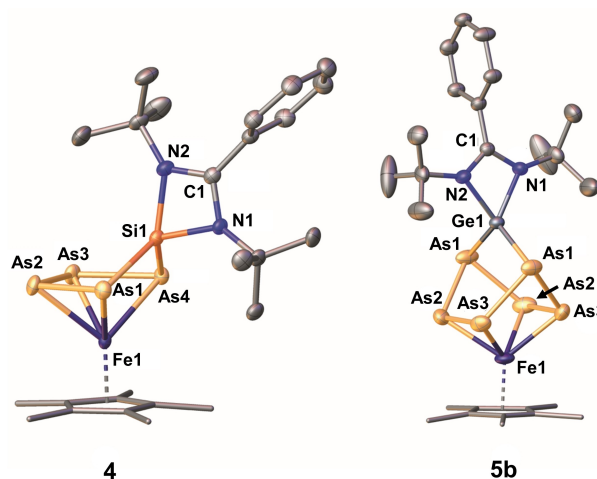


**Figure 3.** Molecular structure of **4** and **5b** in the solid state. Hydrogen atoms are omitted for clarity. The Cp\* ligands are drawn in a wire frame model. Thermal ellipsoids are drawn at 50% probability.



first norbornadiene-like  $\text{As}_6\text{SiL}$  ligand stabilized in the coordination sphere of transition metals.

The reaction of the dimeric germylene  $(\text{LGe})_2$  ( $\text{L} = \text{PhC}(\text{N}^t\text{Bu})_2$ ) with **I** affords the isostructural (to **5a**) Ge derivative  $[\text{Cp}^*\text{Fe}(\eta^4\text{-As}_6\text{GeL})]$  (**5b**). However, the resulting red reaction mixture is highly air-, light- and moisture-sensitive.  $^1\text{H}$  NMR spectroscopy of the reaction mixture reveals the formation of several different species, bearing a  $\text{Cp}^*$ - or *tert*-butyl-containing unit (Figure S22). Utilizing the different solubilities of the given products (cf. Supporting Information for workup), single crystals of **5b** were obtained from a solution of THF layered with *n*-pentane and stored at 8 °C under the exclusion of light. Unfortunately, no other species could be unambiguously identified. Notably, (LIF-DI) mass spectrometry does not show any peaks, instead the formation of a solid (presumably germanium or arsenic) was observed blocking the canula.

Nevertheless, complex **5b** was obtained as brown blocks in 17 % yield after consecutive workup (cf. SI) as the solely isolatable product. Single crystals X-ray structure analysis of **5b** reveals an isostructural motif to **5a**, when silicon (**5a**) is replaced by germanium (**5b**) (Figure 3). The respective Ge–As bond lengths of 2.3775(8) – 2.3876(3) Å indicate the presence of a single to double bond character.<sup>[18,19]</sup> Thus, pentaarsaferrocene **I** can be used as a polyarsenic source to form the unprecedented norbornadiene-like germylene-polyarsanide complex **5b**, representing the first compound of its kind.

## Conclusion

In summary, the polyarsenic complex  $[\text{Cp}^*\text{Fe}(\eta^5\text{-As}_5)]$  (**I**) was demonstrated as to be a valuable starting material for the synthesis of arsenic-rich carbene, silylene, and germylene ligand complexes. This way, novel neutral polyarsenic-NHC-adduct complexes were accessible (**1a**, **1b**). Moreover, the reaction of **I** with  $\text{Et}^i\text{CAAC}$  leads to fragmentation, and a unique CAAC-stabilized  $\text{As}_6$  sawhorse molecule  $[\text{As}_2(\text{As}^i\text{CAAC})_4]$  (**2**) is formed. Furthermore, the reaction of **I** with dimeric silylenes/germylenes  $(\text{LE})_2$  ( $\text{E} = \text{Si}, \text{Ge}$ ) leads to unique mixed cyclic polyarsenic-silicon complexes ( $[\text{Cp}^*\text{Fe}(\eta^4\text{-As}_4\text{SiL})]$  **4**,  $[\text{Cp}^*\text{Fe}(\eta^4\text{-As}_6\text{SiL})]$  **5a**) with unprecedented  $\text{As}_5\text{Si}$  six-membered rings and a first polyarsenic-germanium compound  $[\text{Cp}^*\text{Fe}(\eta^4\text{-As}_6\text{GeL})]$  (**5b**). All in all, **I** paves the way for a variety of novel group 14 arsenic ligand complexes with rare to novel structural motifs and exhibits a very different reaction behavior than the one found for the lighter homolog  $[\text{Cp}^*\text{Fe}(\eta^5\text{-P}_5)]$  (**II**).<sup>[16]</sup>

## Experimental Section

Experimental procedures, full analytical data<sup>[22]</sup> and details regarding quantum chemical calculations are described in the Supporting Information.

## Acknowledgements

This work was supported by the Deutsche Forschungsgemeinschaft within the projects 408306858: Sche 384/38-3 and 470309834: RO 2008/21-1 and Sche 384/45-1. S.R. and C.R. are grateful to the Studienstiftung des Deutschen Volkes for PhD fellowships. Open Access funding enabled and organized by Projekt DEAL.

## Conflict of Interest

The authors declare no conflict of interest.

## Data Availability Statement

The data that support the findings of this study are available in the supplementary material of this article.

**Keywords:** Arsenic · Functionalization · Germylene · Nucleophiles · Silylene

- [1] A. J. Arduengo, III, R. L. Harlow, M. Kline, *J. Am. Chem. Soc.* **1991**, *113*, 361–363.
- [2] a) M. N. Hopkinson, C. Richter, M. Schedler, F. Glorius, *Nature* **2014**, *510*, 485–496; b) V. Nesterov, D. Reiter, P. Bag, P. Frisch, R. Holzner, A. Porzelt, S. Inoue, *Chem. Rev.* **2018**, *118*, 9678–9842; c) D. Zhao, L. Candish, D. Paul, F. Glorius, *ACS Catal.* **2016**, *6*, 5978–5988.
- [3] V. Lavallo, Y. Canac, C. Präsang, B. Donnadiou, G. Bertrand, *Angew. Chem. Int. Ed.* **2005**, *44*, 5705–5709.
- [4] a) C.-W. So, H. W. Roesky, J. Magull, R. B. Oswald, *Angew. Chem. Int. Ed.* **2006**, *45*, 3948–3950; b) S. S. Sen, H. W. Roesky, D. Stern, J. Henn, D. Stalke, *J. Am. Chem. Soc.* **2010**, *132*, 1123–1126; c) S. Inoue, J. D. Epping, E. Irran, M. Driess, *J. Am. Chem. Soc.* **2011**, *133*, 8514–8517; d) S. Nagendran, S. S. Sen, H. W. Roesky, D. Koley, H. Grubmüller, A. Pal, R. Herbst-Irmer, *Organometallics* **2008**, *27*, 5459–5463; e) S. S. Sen, A. Jana, H. W. Roesky, C. Schulzke, *Angew. Chem. Int. Ed.* **2009**, *48*, 8536–8538.
- [5] W. W. Schoeller, *Phys. Chem. Chem. Phys.* **2009**, *11*, 5273–5280.
- [6] a) M. Scheer, G. Balázs, A. Seitz, *Chem. Rev.* **2010**, *110*, 4236–4256; b) D. J. Scott, J. Cammarata, M. Schimpf, R. Wolf, *Nat. Chem.* **2021**, *13*, 458–464; c) D. Sarkar, C. Weetman, D. Munz, S. Inoue, *Angew. Chem. Int. Ed.* **2021**, *60*, 3519–3523; d) M. M. D. Roy, A. Heilmann, M. A. Ellwanger, S. Aldridge, *Angew. Chem. Int. Ed.* **2021**, *60*, 26550–26554.
- [7] a) C. D. Martin, C. M. Weinstein, C. E. Moore, A. L. Rheingold, G. Bertrand, *Chem. Commun.* **2013**, *49*, 4486–4488; b) J. D. Masuda, W. W. Schoeller, B. Donnadiou, G. Bertrand, *J. Am. Chem. Soc.* **2007**, *129*, 14180–14181; c) O. Back, G. Kuchenbeiser, B. Donnadiou, G. Bertrand, *Angew. Chem. Int. Ed.* **2009**, *48*, 5530–5533; d) J. D. Masuda, W. W. Schoeller, B. Donnadiou, G. Bertrand, *Angew. Chem. Int. Ed.* **2007**, *46*, 7052–7055.
- [8] S. S. Sen, S. Khan, H. W. Roesky, D. Kratzert, K. Meindl, J. Henn, D. Stalke, J.-P. Demers, A. Lange, *Angew. Chem. Int. Ed.* **2011**, *50*, 2322–2325.
- [9] Y. Xiong, S. Yao, M. Brym, M. Driess, *Angew. Chem. Int. Ed.* **2007**, *46*, 4511–4513.

- [10] R. P. Tan, N. M. Comerlato, D. R. Powell, R. West, *Angew. Chem. Int. Ed.* **1992**, *31*, 1217–1218.
- [11] A. E. Seitz, M. Eckhardt, S. S. Sen, A. Erlebach, E. V. Peresyphina, H. W. Roesky, M. Sierka, M. Scheer, *Angew. Chem. Int. Ed.* **2017**, *56*, 6655–6659.
- [12] A. E. Seitz, M. Eckhardt, A. Erlebach, E. V. Peresyphina, M. Sierka, M. Scheer, *J. Am. Chem. Soc.* **2016**, *138*, 10433–10436.
- [13] S. Yao, Y. Grossheim, A. Kostenko, E. Ballester-Martínez, S. Schutte, M. Bispinghoff, H. Grützmacher, M. Driess, *Angew. Chem. Int. Ed.* **2017**, *56*, 7465–7469.
- [14] M. Haimerl, C. Schwarzmaier, C. Riesinger, A. Y. Timoshkin, M. Melaimi, G. Bertrand, M. Scheer, *Chem. Eur. J.* **2023**, *29*, e202300280.
- [15] F. Riedlberger, S. Todisco, P. Mastrorilli, A. Y. Timoshkin, M. Seidl, M. Scheer, *Chem. Eur. J.* **2020**, *26*, 16251–16255.
- [16] R. Yadav, T. Simler, S. Reichl, B. Goswami, C. Schoo, R. Köppe, M. Scheer, P. W. Roesky, *J. Am. Chem. Soc.* **2020**, *142*, 1190–1195.
- [17] R. Yadav, B. Goswami, T. Simler, C. Schoo, S. Reichl, M. Scheer, P. W. Roesky, *Chem. Commun.* **2020**, *56*, 10207–10210.
- [18] P. Pyykkö, M. Atsumi, *Chem. Eur. J.* **2009**, *15*, 186–197.
- [19] P. Pyykkö, M. Atsumi, *Chem. Eur. J.* **2009**, *15*, 12770–12779.
- [20] A. B. Rozhenko, A. Ruban, V. Thelen, M. Nieger, K. Airola, W. W. Schoeller, E. Niecke, *Eur. J. Inorg. Chem.* **2012**, 2502–2507.
- [21] for an As<sub>3</sub>SiL-ligand cf.: M. Piesch, S. Reichl, M. Seidl, G. Balázs, M. Scheer, *Angew. Chem. Int. Ed.* **2021**, *60*, 15101–15108.
- [22] Deposition numbers 2279222 (**1a**), 2279223 (**1b**), 2279224 (**2**), 2279225 (**3**), 2279226 (**4**), 2279227 (**5a**), 2279228 (**5b**) and 2280384 [Cp\*Fe(η<sup>4</sup>-P<sub>5</sub>)<sup>Et</sup>CAAC] (**1'**) contain the supplementary crystallographic data for this paper. These data are provided free of charge by the joint Cambridge Crystallographic Data Centre and Fachinformationszentrum Karlsruhe Access Structures service.

Manuscript received: October 24, 2023

Accepted manuscript online: November 20, 2023

Version of record online: December 20, 2023